# ACCELERATED IRRADIATION TESTING OF MINIATURE NUCLEAR FUEL AND CLADDING SPECIMENS

C.M. PETRIE, T. KOYANAGI, R.H. HOWARD, K.G. FIELD, J.R. BURNS, K.A. TERRANI
*Oak Ridge National Laboratory*
*P.O. Box 2008, Oak Ridge, TN 37831, USA*

## ABSTRACT

Qualification of advanced nuclear fuels and materials requires irradiation testing to provide input to predictive models for licensing. Oak Ridge National Laboratory has a long history of performing accelerated irradiation testing and post-irradiation examination (PIE) of miniature material specimens to determine the evolution of microstructure and thermophysical properties, leveraging the High Flux Isotope Reactor, dedicated hot cells, and instruments for handling small, low-level radioactive samples. This work gives a brief overview of irradiation testing of miniature samples to support qualification of advanced fuel cladding materials such as FeCrAl alloys and SiC ceramic matrix composites. More recent work has enabled separate effects irradiation testing of miniature fuel specimens. The small fuel size essentially decouples fuel temperature from fission rate, allowing for highly accelerated testing without large temperature gradients. This paper briefly highlights the new mini fuel irradiation facility and its first set of experiments.

## 1. Introduction

The Advanced Fuels Campaign within the US Department of Energy (DOE) Office of Nuclear Energy is considering a variety of advanced nuclear fuels and fuel cladding materials for use in light water reactors (LWRs) and/or advanced reactor concepts [1-3]. These advanced fuels and materials could provide increased safety margins under accident scenarios, improved fission product retention, reduced steam oxidation kinetics (for LWR applications), and improved neutron economy during normal operation. Qualification of any new nuclear fuel or material requires rigorous irradiation testing under expected in-service conditions and a sound fundamental understanding of irradiation performance. Because of the large number of variables that affect fuel and material performance (temperature, dose, composition, processing, etc.), there is a strong interest in building the capability to rapidly test a large matrix of fuel or materials in an economical manner. Clearly, an Edisonian approach involving numerous sequential integral fuel testing to cover all possible fuel performance variables is not possible within limited research and development budgets and timeframes.

This paper briefly highlights a few specific examples of how the unique facilities at Oak Ridge National Laboratory (ORNL) are being used to improve the fundamental understanding of irradiation effects on advanced fuel cladding materials such as FeCrAl alloys and silicon carbide (SiC) fibre–reinforced SiC matrix composites (SiC/SiC composites). The paper also highlights the new mini fuel irradiation facility and the first experiments that have been initiated.

This facility allows for high throughput, low-cost, separate effects irradiation testing of a wide range of advanced fuel concepts. Both fuel and materials irradiations leverage miniaturized test specimens to allow for accelerated irradiation testing with reduced component activation, allowing for handling outside a hot cell and the use of advanced characterization techniques.

## 2. Miniature irradiation facilities

ORNL is home to the High Flux Isotope Reactor (HFIR), which provides one of the highest steady-state neutron fluxes in the world. This reactor allows for highly accelerated irradiation testing of nuclear fuel and materials that can be examined on-site in dedicated hot cells and other post-irradiation examination (PIE) facilities. The HFIR's extremely high power density comes at a cost of reduced space for experiments. Therefore, ORNL researchers strive to reduce the size of experiments and test specimens through novel experiment design concepts and PIE techniques to measure various phenomena at ever decreasing length scales.

### 2.1 Materials irradiations

Materials irradiations in HFIR are typically conducted in small (Ø11 mm × 65 mm length), sealed aluminium "rabbit" capsules. These rabbits can be transferred in and out of the reactor core via a hydraulic tube or placed in permanent positions within the centre flux trap (the region with the highest fast and thermal neutron flux) of the reactor. Peak values (depending on the exact location within the flux trap) for the thermal neutron flux, fast neutron flux, displacements per atom (dpa) rate in stainless steel, and gamma heating rate in stainless steel are $2.5 \times 10^{15}$ n/cm2/s, $1.1 \times 10^{15}$ n/cm$^2$/s, 0.0035 dpa/hour, and 40 W/g, respectively. Most materials irradiation experiments in the flux trap are not instrumented. Instead, passive SiC thermometers are used to evaluate the irradiation temperature post-irradiation using dilatometry [4].

Figure 1 shows three examples of materials irradiation capsules with varying complexity. Figure 1 (a) shows an example of a rabbit containing miniature flat-sheet, dog-bone tensile specimens (SS-J2, SS-J3, or SS-2E geometry). These rabbits are routinely irradiated at temperatures ranging from 200–800°C. Sub-miniature geometries allow up to 32 specimens to be irradiated in a single rabbit capsule. The addition of the SS-2E geometry further reduces the specimen dimensions from 16 mm × 4 mm × 0.5 mm thick with a 5 mm × 1.2 mm gauge section (SS-J2) to 7 mm × 2.6 mm × 0.4 mm thick with a 3.55 mm × 0.8 mm gauge section. This new geometry maximizes specimen loading in the limited volume of a rabbit and minimizes specimen radioactivity to the extent that advanced out-of-cell characterization techniques such as digital image correlation or in-situ electron backscatter diffraction can be used [5]. While the current irradiation capsule only allows for dry irradiation conditions, a separate vehicle has been designed to allow for irradiation of materials specimens in a thermosyphon (closed system) with circulating water (either PWR or boiling water reactor coolant chemistry) by taking advantage of natural circulation [6].

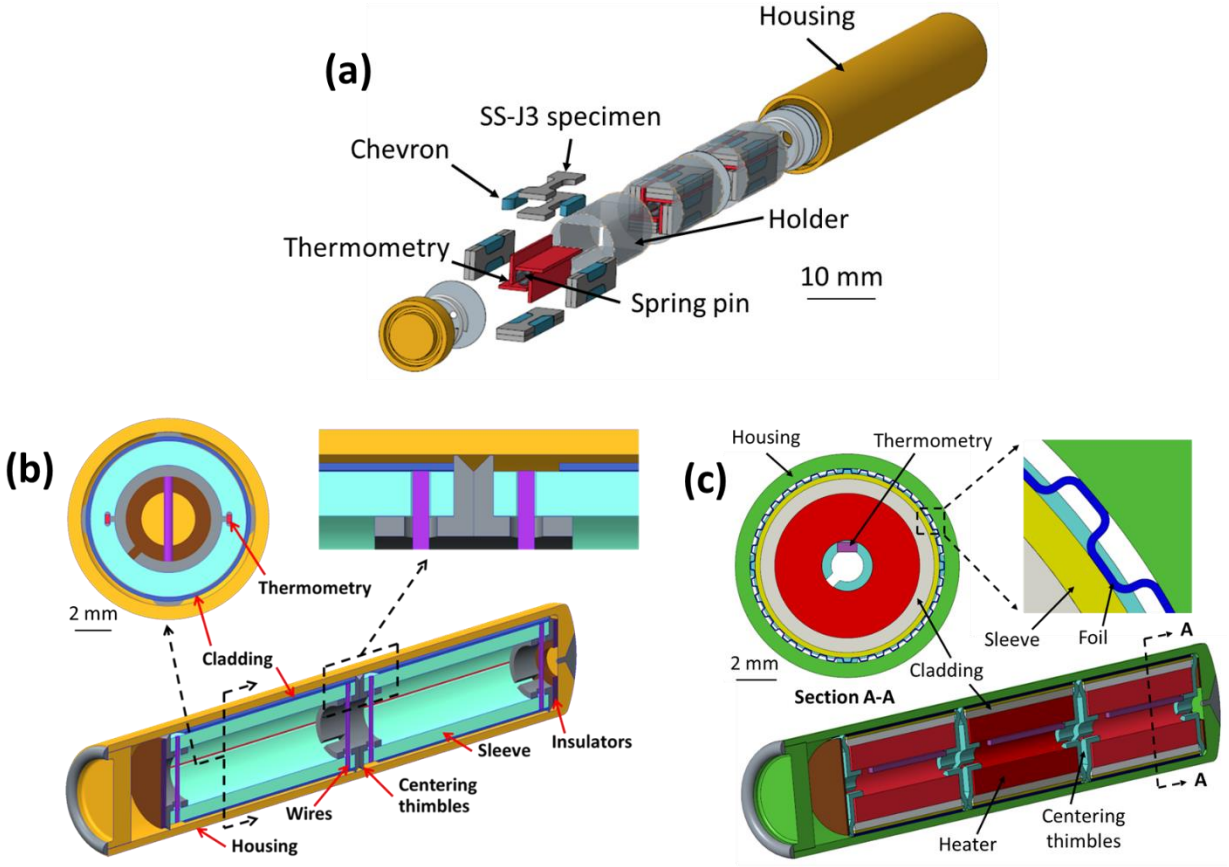


Fig 1. Rabbit designs for (a) sub-miniature flat tensile specimen irradiations, (b) shortened PWR cladding tube irradiations, and (c) SiC/SiC composite cladding tube irradiations under a relevant LWR heat flux.

Figure 1 (b) shows a standard rabbit design for irradiating pressurized water reactor (PWR) fuel cladding, with representative diameter and thickness for typical 17 × 17 array cladding [7, 8]. Shortened cladding tube sections must be used to fit inside the limited volume of a rabbit. This simple design allows for measurement of mechanical properties and microstructure evolution of cladding tubes with representative geometry and pre-irradiation microstructure during accelerated irradiation testing at typical LWR temperatures. This design is useful for performing low-cost evaluations of the irradiation performance of coated fuel cladding concepts for improved resistance to corrosion and wear [9].

Figure 1 (c) shows a novel rabbit concept for irradiating miniature SiC/SiC composite tube specimens for potential fuel cladding applications in LWRs [10, 11]. The shortened cladding tube diameters (8.5 mm × 0.7 mm thick) are slightly reduced to fit inside a standard rabbit capsule. However, this design allows for testing of SiC/SiC cladding tubes under a representative high radial heat flux (~0.6 MW/m$^2$) and surface temperature (300−350°C) without the complexity of a fuelled experiment. This is made possible by the HFIR's extremely high gamma heating rates. Gamma heat generated in a dense molybdenum heater inside the cladding tube passes radially through the cladding thickness. The cladding is surrounded by a thin aluminium sleeve and a corrugated aluminium foil which compresses as the cladding tube swells under irradiation. With this configuration, the cladding is subject to the differential swelling stresses that would be expected during LWR in-service conditions. Ongoing work is in process to quantify this swelling-induced stress and its effect on thermal/mechanical properties and gas hermeticity.

## 2.2 Fuels irradiations

While most materials irradiations use rabbit capsules inside the HFIR's flux trap, fuels irradiations are typically conducted in the reactor's beryllium reflector. This is because the extremely high thermal neutron flux in the flux trap results in prohibitively high fuel heating rates, even with the use of depleted uranium. While integral irradiation testing of full-size LWR fuel pellets has been performed in the HFIR using thermal neutron shielded facilities [12], more recent efforts have focused on highly accelerated irradiation testing of extremely small (<4 $mm^3$) mini fuel specimens [13-15], as shown in Figure 2. The fuel's reduced size eliminates any concern regarding spatial neutron flux gradients in the reflector positions, as gradients occur over much larger distances compared to the size of the fuel. The mini fuel facility allows for decoupling of the fission rate from the fuel temperature, rapid accumulation of burnup without prohibitively large temperature gradients, and reduced concerns regarding fuel activation. The HFIR's high thermal neutron flux also allows for greatly reduced fuel enrichment. In fact, even with depleted uranium, fission of $^{239}Pu$—bred from (n,g) reactions in $^{238}U$—eventually results in equilibrium fuel heating rates that are approximately 4 times greater than a typical LWR on a per unit mass basis. While Figure 2 shows fuel with kernel geometry, the design can accommodate a wide range of fuel geometries including coated fuel particles of varying sizes, disk geometry, or even a miniaturized fuel pin.

PIE of mini fuel specimens will include fission gas release, volumetric swelling, and microstructural characterization. Fuel specimens are individually encapsulated to allow for puncturing of capsules and cold trapping of gaseous fission products. Swelling can be measured using x-ray computed tomography or pycnometry (gas or mercury).

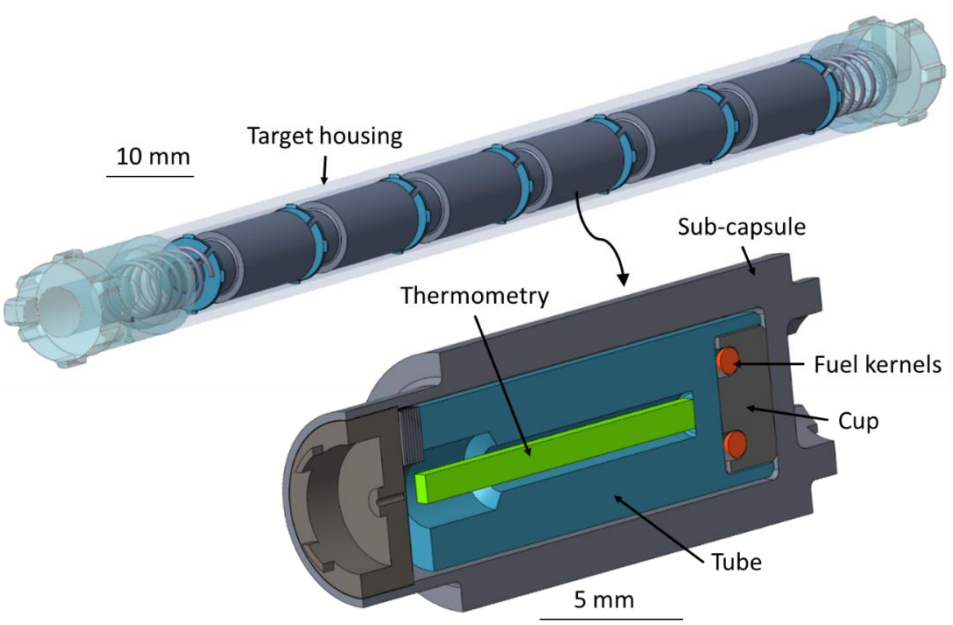


Fig 2. Mini fuel target and sub-capsule

# 3. Results

## 3.1 Metal cladding irradiations

The flexible rabbit design that was developed to allow economical testing of small SS-J-style tensile specimens was leveraged to aid in understanding the effects of composition,

temperature, and dose on the tensile properties of irradiated FeCrAl alloys for LWR applications. Table 1 summarizes the testing performed to date on irradiated FeCrAl alloys, with references that provide more detail. The reported irradiation temperatures are the average temperatures of at least 5 separate passive SiC temperature monitors evaluated using a previously established technique [4]. The uncertainties represent the standard deviation of the temperatures, which varied from as low as 1°C to as high as 38°C. In general, the FCAY capsule series evaluated the effects of varying Cr and Al content in model and commercial alloys on the irradiation performance (e.g., hardening, embrittlement) at LWR temperatures for doses covering the range expected for a typical fuel assembly. The FCAT series is now evaluating the performance of engineering grade alloys with refined composition based on the initial data gathered during the FCAY campaign. The FCAT series is evaluating both temperature and dose dependence over a much smaller range of alloy composition. The large amount of data that has been acquired on irradiated FeCrAl alloys has moved this class of alloys from the conceptual stage to deployment of lead test rods and lead test assemblies in just 6 years. This accomplishment exemplifies the value of the accelerated, economical irradiation testing of miniature specimens that can be performed in the HFIR.

| Capsule ID | Samples | Dose (dpa) | Irradiation Temperature (°C) | References |
|---|---|---|---|---|
| FCAY-01 | Model and commercial alloys with 10–22 wt% Cr, 3–5 wt% Al, varying minor alloying additions (e.g. $Y_2O_3$) | 0.3 | 335 ± 1 | [16-23] |
| FCAY-02 | | 0.8 | 355 ± 3 | |
| FCAY-03 | | 1.8 | 382 ± 5 | |
| FCAY-04 | | 7 | 320 ± 10 | |
| FCAY-05 | | 13.8 | 341 ± 26 | |
| FCAT-01 | Engineering grade alloys with 10–13 wt% Cr, 5–7 wt% Al, varying minor alloying additions ($Y_2O_3$, Mo, Nb, TiC) | 1.9 | 195 ± 38 | [22, 24, 25] |
| FCAT-02 | | 1.8 | 363 ± 21 | |
| FCAT-03 | | 1.9 | 559 ± 28 | |
| FCAT-04 | Engineering grade alloys with 10-13 wt% Cr, 5-7 wt% Al, varying minor alloying additions ($Y_2O_3$, Mo, Nb, TiC) | 8.3 | 200* | Capsules have completed irradiation and are awaiting disassembly and PIE |
| FCAT-05 | | 7.9 | 330* | |
| FCAT-06 | | 8.3 | 550* | |
| FCAT-07 | Engineering grade alloys with 10-13 wt% Cr, 5-7 wt% Al, varying minor alloying additions ($Y_2O_3$, Mo, Nb, TiC) | 16.3 | 200* | |
| FCAT-08 | | 15.4 | 330* | |
| FCAT-09 | | 16.3 | 550* | |
| * Nominal target temperature | | | | |

Tab 1: Summary of irradiation testing of FeCrAl alloys performed at ORNL

Recent work has demonstrated that the SS-J specimen geometry can be even further reduced in size to the point that some specimens have low enough activity after irradiation that they can be examined using advanced characterization techniques such as digital image correlation (DIC) [5, 26]. DIC offers the ability to perform two-dimensional strain mapping and can obtain true stress – true strain curves. A reduced specimen size also allows for a higher specimen loading inside the limited space of materials irradiation capsules.

While flat-sheet tensile specimens are useful for scoping studies to determine the effects of variables such as temperature, composition, processing, and dose, ultimately, LWR fuel

performance codes require tensile properties for thin-walled tube geometries. For this reason, ORNL initiated a series of rabbit irradiations to test shortened cladding tube specimens with representative 17 × 17 array PWR diameter, thickness, and microstructure [8]. The primary PIE activity will be to determine hoop tensile properties after machining ring specimens from the tubes so that the specimen geometry is similar to what has been done previously for unirradiated material [27].

## 3.2 Ceramic cladding irradiations

The capability to test miniature SiC/SiC cladding tubes during irradiation under high radial heat flux has enabled economical testing of a wide variety of cladding architectures, including composite materials from General Atomics (GA) and the Commissariat à l'énergie atomique et aux énergies alternatives (CEA), chemical vapor deposition (CVD) monolith tubes from The Dow Chemical Company, and duplex specimens with an inner monolith and outer composite provided by GA and the Korea Atomic Energy Research Institute (KAERI). Some of the cladding tubes were coated with various environmental barrier coatings that were proposed to prevent hydrothermal corrosion in certain types of water chemistry [28]. Specimens with Cr, CrN, and TiN have been irradiated using this experiment design. All tubes were irradiated to a dose of 2 dpa while maintaining a cladding surface temperature of approximately 325°C.

PIE of the irradiated cladding tubes is ongoing. The examinations will include nondestructive evaluation using x-ray computed tomography (XCT) to observe any internal cracking, resonant ultrasound spectroscopy to determine irradiation effects on elastic constants [29], and gas permeability measurements [30]. Other work will involve (1) destructive c-ring testing or other methods to determine residual stresses that developed in cladding tubes due to differential swelling and (2) comparison of those stresses with thermomechanical simulations [31].

Some initial observations of the cladding response to irradiation under a high radial heat flux have been gathered. Figure 3 shows an image obtained from XCT of an irradiated specimen. Both axial and radial cracks can be observed after irradiation. While XCT was not performed on the exact same specimen before and after irradiation, XCT of specimens prepared under the same condition shows that axial cracks were also present in the unirradiated specimens. Therefore, it is not clear whether the axial cracks were caused by irradiation. Radial cracks can be seen on the inner surface of the cladding. These cracks were not observed in any of the unirradiated specimens, and therefore the radial cracks may have been caused by irradiation. The fact that the radial cracks originated on the inner surface of the cladding is consistent with the expected stress state in the cladding with near equi-biaxial (in the hoop and axial directions) tensile stress on the inner surface and near equi-biaxial compressive stress on the outer surface due to the inverse temperature-dependence of swelling in SiC [32]. It is expected that the high tensile stress (on the order of 150 MPa), which is beyond the proportional limit strength for typical SiC/SiC composites, was enough to initiate a crack. However, the transition to compressive stress toward the outer cladding surface prevented the crack from propagating through the cladding thickness. While the XCT images do not give quantitative information regarding the stress state in the cladding after irradiation, they do give confidence that the separate effects testing can adequately represent in-core conditions and the observed cracking qualitatively matches thermomechanical simulations. Future work involving c-ring testing or other methods will be used to provide quantitative information regarding the cladding stresses after irradiation.

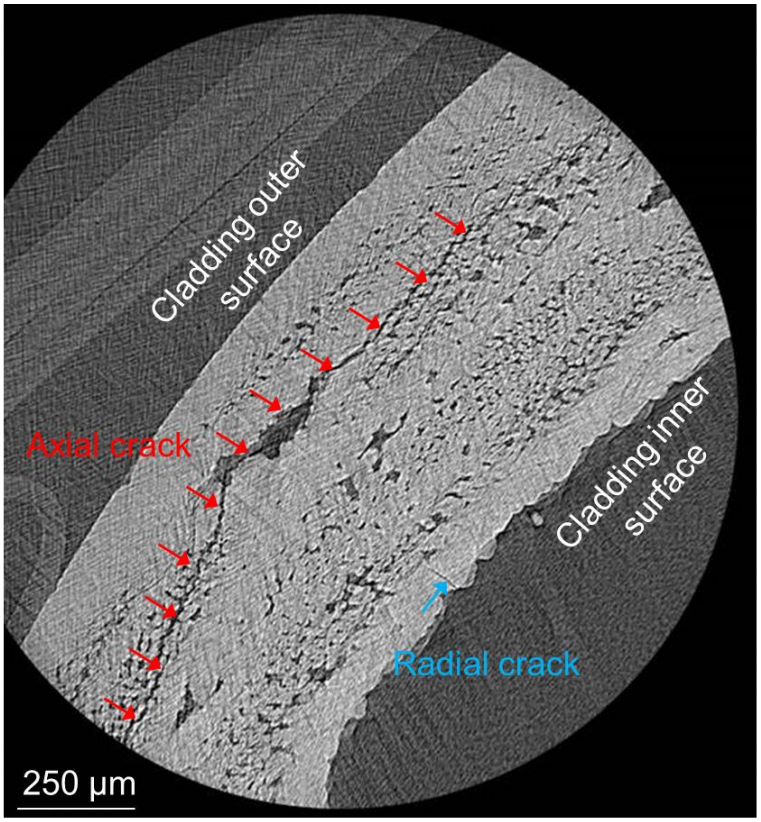

Fig 3. X-ray image showing radial and axial cracks in a SiC/SiC composite tube after irradiation under a high radial heat flux

### 3.3 Fuel irradiations

Table 2 summarizes the test matrix for the first set of mini fuel irradiation experiments that tests UN kernels and UN-bearing tristructural-isotropic (TRISO) particles. More details regarding the fuel fabrication can be found in other works [33]. This fuel is being irradiated at low temperatures (450−550°C) relevant to LWR applications. Most if not all of the irradiation performance data generated for UN fuel to date have come from higher temperature testing (800−1,600°C) relevant to advanced reactors [34].

The high neutron flux in the HFIR would result in extremely high fission rates if $^{235}$U enrichments of 4−5% were used. However, with depleted or natural uranium the fuel heating rate is low at the beginning of the irradiation but quickly approaches an equilibrium value of ~160 W/g once an equilibrium is achieved between breeding of $^{239}$Pu from transmutation of $^{238}$U and fission of the $^{239}$Pu. Furthermore, heating rates in the fuel and the surrounding components vary over the course of a HFIR cycle as the reactor control plates are withdrawn from the core. More detail regarding the neutronics analyses for the experiment can be found in previous works [13-15]. Thermal analyses were performed to predict temperature distributions within the fuel specimens at the beginning of the first cycle of irradiation when heating rates are lowest and at the end of a HFIR cycle once the fission rate approaches an equilibrium value. These thermal simulations are essential to understanding the irradiation conditions over the entire duration of the experiment. Combining the temperature and burnup history with post-irradiation measurements of fuel swelling and fission gas release will help predict full-scale fuel performance during expected in-service conditions. Figure 4 shows expected temperatures within one of the fuel kernels. Expected temperature gradients within the fuel kernels are less than 23°C. Fuel temperatures at the beginning of the irradiation with

depleted uranium are closer to 450°C because there has not yet been sufficient time to allow breeding of $^{239}Pu$. These temperature variations are much smaller than those that are present during typical integral fuel testing due to the larger pellet size and the resulting strong coupling between fuel temperature and fission rate.

| Fuel form | Kernel theoretical density | $^{235}U$ Enrichment (wt %) | Target burnup (% FIMA) |
|---|---|---|---|
| $UC_{0.20}N_{0.80}$ kernels | 94.9% | 0.22% | 1%, 6% |
| $UC_{0.15}N_{0.85}$ kernels | 90.6% | 0.71% | |
| $UC_{0.20}N_{0.80}$ kernels | 90.9% | 0.22% | |
| $U_{0.89}Gd_{0.11}C_{0.11}N_{0.89}$ kernels | 92.0% | 0.71% | |
| $U_{0.98}Gd_{0.02}C_{0.15}N_{0.85}$ kernels | 93.6% | 0.71% | |
| $UC_{0.20}N_{0.80}$ TRISO particles | 87.2% | 0.22% | |

Tab 2: Test matrix for first set of mini fuel experiments using UN kernels and TRISO particles

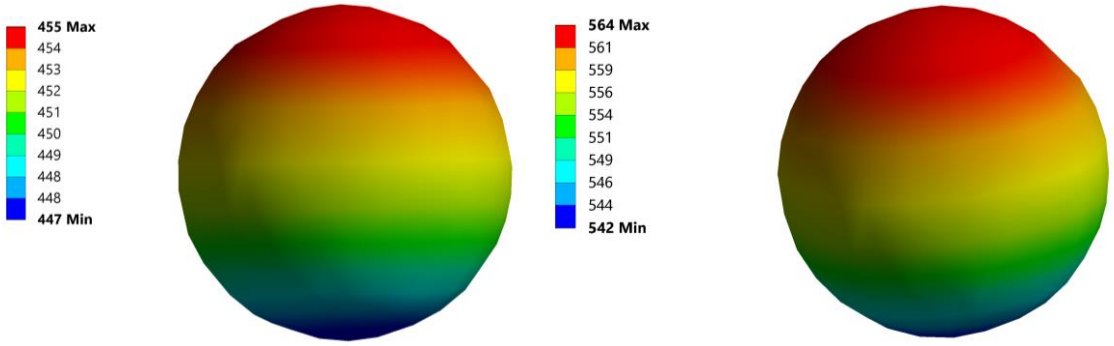


Fig 4. Calculated temperature distribution (in °C) within a single UN fuel kernel at the beginning of the first cycle of irradiation (left) and at the end of cycle once the fuel fission heating rate has reached an equilibrium value of 160 W/g (right)

The mini fuel experiments described in this work will also allow for examination of the effects of impurities (e.g., carbon), density, and burnable absorbers (Gd) at two different burnup levels within a single irradiation campaign. Loose TRISO particles are also being irradiated under more controlled conditions compared to previous work that tested large numbers of particles compacted in a graphite matrix [35, 36]. Traditionally, evaluating the effects of impurity content, density, and burnable absorber content at two different burnup levels would require at least six integral fuel tests, each of which would cost far more than this first set of mini fuel experiments. This demonstrates how valuable the mini fuel test capability can be, particularly during the early stages of development of an advanced fuel.

## 4. Summary

This paper summarizes some of ORNL's unique facilities and capabilities being used to improve the fundamental understanding of irradiation effects on advanced fuel cladding materials such as FeCrAl alloys and SiC/SiC ceramic matrix composites, as well as advanced nuclear fuels. The ability to perform separate effects testing on miniature specimens helps reduce experiment complexity and cost. Reducing specimen size also decreases neutron activation, which can enable the use of advanced characterization techniques located in radiological facilities outside a hot cell. The HFIR's extremely high-power density allows for

highly accelerated testing. Combining the high neutron flux with miniaturized test specimens allows for rapid accumulation of fuel burnup without prohibitively large temperature gradients. A few current irradiation testing campaigns are briefly summarized to give an idea of the type of data that can be generated to support qualification of new fuels and materials.

## 5. Acknowledgements

This research was supported by the Advanced Fuels Campaign and the Nuclear Science User Facilities Program of the U.S. Department of Energy (DOE), Office of Nuclear Energy. Neutron irradiation in the HFIR was made possible by the DOE Office of Basic Energy Sciences.

## 6. References

[1] S. J. Zinkle, et al., "Accident tolerant fuels for LWRs: A perspective", Journal of Nuclear Materials, Vol. 448, pp. 374–379, 2014.

[2] J. Carmack, et al., "Overview of the U.S. DOE Accident Tolerant Fuel Development Program," Proceedings of Top Fuel 2013, Charlotte, NC, 2013.

[3] K. A. Terrani, "Accident tolerant fuel cladding development: Promise, status, and challenges", Journal of Nuclear Materials, Vol. 501, pp. 13-30, 2018.

[4] A. Campbell, et al., "Method for analyzing passive silicon carbide thermometry with a continuous dilatometer to determine irradiation temperature", Nuclear Instruments and Methods in Physics Research B, Vol. 370, pp. 49–58, 2016.

[5] M. N. Gussev, et al., "Sub-size tensile specimen design for in-reactor irradiation and post-irradiation testing", Nuclear Engineering and Design, Vol. 320, pp. 298-308, 2017.

[6] J. McDuffee, N. Patel, and J. Carbajo, "Operational Possibilities of a Thermosyphon Facility for Fuels and Materials Irradiation," 40th Enlarged Halden Programme Group Meeting, Lillehammer, Norway, 2017.

[7] C. M. Petrie, et al., "Analysis and Experimental Qualification of an Irradiation Capsule Design for Testing Pressurized Water Reactor Fuel Cladding in the High Flux Isotope Reactor," Oak Ridge National Laboratory, Oak Ridge, TN, ORNL/TM-2017/67, 2017.

[8] C. M. Petrie, K. G. Field, and K. Linton, "Irradiation of Wrought FeCrAl Tubes in the High Flux Isotope Reactor," Oak Ridge National Laboratory, Oak Ridge, TN, ORNL/SR-2017/466, 2017.

[9] J. Bischoff, et al., "AREVA NP's enhanced accident-tolerant fuel developments: Focus on Cr-coated M5 cladding", Nuclear Engineering and Technology, Vol. 50, pp. 223-228, 2018.

[10] C. M. Petrie, et al., "Experimental design and analysis for irradiation of SiC/SiC composite tubes under a prototypic high heat flux", Journal of Nuclear Materials, Vol. 491, pp. 94–104, 2017.

[11] C. M. Petrie and T. Koyanagi, "Assembly and Delivery of Rabbit Capsules for Irradiation of Silicon Carbide Cladding Tube Specimens in the High Flux Isotope Reactor," Oak Ridge National Laboratory, Oak Ridge, TN, ORNL/TM-2017/433, 2017.

[12] L. J. Ott, et al., "Irradiation of SiC Clad Fuel Rods in the HFIR," Proceedings of Top Fuel 2013, Charlotte, NC, 2013.

[13] C. M. Petrie, et al., "Miniature Fuel Irradiations in the High Flux Isotope Reactor," 40th Enlarged Halden Programme Group Meeting, Lillehammer, Norway, 2017.

[14] C. M. Petrie, et al., "Small-Scale Fuel Irradiation Testing in the High Flux Isotope Reactor," Water Reactor Fuel Performance Meeting 2017, Jeju Island, Korea, 2017.

[15] C. M. Petrie, et al., "Irradiation of Miniature Fuel Specimens in the High Flux Isotope Reactor," Oak Ridge National Laboratory, Oak Ridge, TN, ORNL/SR-2018/844, 2018.

[16] D. Zhang, S. A. Briggs, and K. G. Field, "Role of refractory inclusions in the radiation-induced microstructure of APMT", Journal of Nuclear Materials, Vol. 505, pp. 165-173, 2018.

[17] K. G. Field, K. C. Littrell, and S. A. Briggs, "Precipitation of α′ in neutron irradiated commercial FeCrAl alloys", Scripta Materialia, Vol. 142, pp. 41-45, 2018.

[18] K. G. Field, et al., "Dislocation loop formation in model FeCrAl alloys after neutron irradiation below 1 dpa", Journal of Nuclear Materials, Vol. 495, pp. 20-26, 2017.

[19] K. G. Field, et al., "Mechanical properties of neutron-irradiated model and commercial FeCrAl alloys", Journal of Nuclear Materials, Vol. 489, pp. 118-128, 2017.

[20] S. A. Briggs, et al., "A combined APT and SANS investigation of α′ phase precipitation in neutron-irradiated model FeCrAl alloys", Acta Materialia, Vol. 129, pp. 217-228, 2017.
[21] K. G. Field, et al., "Heterogeneous dislocation loop formation near grain boundaries in a neutron-irradiated commercial FeCrAl alloy", Journal of Nuclear Materials, Vol. 483, pp. 54–61, 2017.
[22] K. G. Field, et al., "Database on Performance of Neutron Irradiated FeCrAl Alloys," Oak Ridge National Laboratory, Oak Ridge, TN, ORNL/TM(2016/335, 2016.
[23] P. D. Edmondson, et al., "Irradiation-enhanced α′ precipitation in model FeCrAl alloys", Scripta Materialia, Vol. 116, pp. 112-116, 2016.
[24] M. N. Gussev, E. Cakmak, and K. G. Field, "Impact of neutron irradiation on mechanical performance of FeCrAl alloy laser-beam weldments", Journal of Nuclear Materials, Vol. 504, pp. 221-233, 2018.
[25] M. N. Gussev and K. G. Field, "Radiation Tolerance of Controlled Fusion Welds in High Temperature Oxidation Resistant FeCrAl Alloys," Oak Ridge National Laboratory, Oak Ridge, TN, ORNL/TM-2017/379; Other: 100619 United States 10.2172/1410934 Other: 100619 ORNL English, 2017.
[26] M. N. Gussev, et al., "Role of Scale Factor During Tensile Testing of Small Specimens," ASTM Sixth International Symposium on Small Specimen Test Techniques, Houston, TX, 2014.
[27] T. M. Link, D. A. Koss, and A. T. Motta, "Failure of Zircaloy cladding under transverse plane-strain deformation", Nuclear Engineering and Design, Vol. 186, pp. 379–394, 1998.
[28] C. Ang, et al., "Evaluation of the First Generation Dual-purpose Coatings for SiC Cladding," Oak Ridge National Laboratory, Oak Ridge, TN, ORNL/TM-2017/318, 2017.
[29] G. Singh, et al., "Evaluating the irradiation effects on the elastic properties of miniature monolithic SiC tubular specimens", Journal of Nuclear Materials, Vol. 499, pp. 107-110, 2018.
[30] X. Hu, et al., "Determination of He and D permeability of neutron-irradiated SiC tubes to examine the potential for release due to micro-cracking," Oak Ridge National Laboratory, Oak Ridge, TN, ORNL-SR-2017/362, 2017.
[31] G. Singh, K. Terrani, and Y. Katoh, "Thermo-mechanical assessment of full SiC/SiC composite cladding for LWR applications with sensitivity analysis", Journal of Nuclear Materials, Vol. 499, pp. 126-143, 2018.
[32] Y. Katoh, et al., "Irradiation – High Heat Flux Synergism in Silicon Carbide Based Fuel Claddings for Light Water Reactors," Top Fuel 2016, Boise, ID, USA, 2016.
[33] J. W. McMurray, et al., "Production of Low-Enriched Uranium Nitride Kernels for TRISO Particle Irradiation Testing," Oak Ridge National Laboratory, Oak Ridge, TN, ORNL/SR-2016/268, 2016.
[34] E. K. Storms, "An equation which describes fission gas release from UN reactor fuel", Journal of Nuclear Materials, Vol. 158, pp. 119–129, 1988.
[35] B. P. Collin, "AGR-1 Irradiation Test Final As-Run Report," Idaho National Laboratory, Idaho Falls, ID, INL/EXT-10-18097, 2015.
[36] P. A. Demkowicz, et al., "Irradiation Performance of AGR-1 High Temperature Reactor Fuel," Proceedings of the HTR 2014, Weihai, China, 2014.